

Use of CFRP/CFCC Reinforcement in Prestressed Concrete Box-Beam Bridges

by Nabil F. Grace, Tsuyoshi Enomoto, Saju Sachidanandan, and Sreejith Puravankara

This paper presents the results of an experimental investigation on the flexural response of two identical box-beam bridge models reinforced and prestressed with different types of carbon fiber reinforced polymer (CFRP) tendons/strands. The first box-beam bridge model BBD-I was reinforced and prestressed using CFRP-DCI tendons, while the second bridge model BBC-I was reinforced and prestressed using carbon fiber composite cable (CFCC) strands. Each box-beam bridge model consisted of two precast prestressed box beams placed adjacent to each other and a CFRP/CFCC reinforced deck slab. The two box beams of each bridge model were prestressed using seven pretensioning tendons/strands and consisted of four transverse diaphragms for transverse post-tensioning. Each box-beam bridge model was also prestressed using 12 longitudinal and four transverse unbonded post-tensioning tendons/strands. The changes in pretensioning forces during and after casting the box beams, ultimate loads and modes of failure, deflections, post-tensioning forces, strains, and energy ratios of both bridge models are presented in this paper. The average values of the measured transfer lengths of 9.5 mm (0.37 in.) diameter CFRP-DCI tendons and 12.5 mm (0.49 in.) diameter CFCC strands were measured as 27.4 times and 22.4 times the nominal strand diameter, respectively. As expected, both bridge models experienced similar failure modes, that is, the failure was initiated by the crushing of concrete in the compression zone followed by the immediate rupture of prestressing tendons/strands. Moreover, it was observed that the ultimate strength of Bridge Model BBD-I was higher and the energy ratio for the same was lower than that of Bridge Model BBC-I. However, the longitudinal unbonded post-tensioning tendons/strands of the two bridge models remained intact even after the complete collapse of the bridge models. In general, both Bridge Models BBD-I and BBC-I experienced identical flexural behavior, especially the cracking load, mode of failure, and variation in post-tensioning forces.

Keywords: beams; bridges; carbon; prestress; reinforcement.

INTRODUCTION

Maintenance of highway superstructures, especially bridge decks, consumes a significant portion of available funds in the U.S. as well as in other countries. In 1999, the U.S. Department of Transportation reported that the U.S. surface infrastructure would need an annual capital of about \$57 billion over the next 20 years to maintain the "1997 performance measure."¹ Corrosion of steel strands/reinforcing bars due to the use of deicing salts and aggressive environmental conditions are the main causes for the deterioration of structures and the loss of structural durability. The use of fibrous composite materials² is now considered to be the best solution to eliminate the corrosion problem associated with conventional steel reinforcement and thereby considerably reducing the maintenance cost of the structures. Some of notable characteristics of composite materials, such as the high strength and stiffness-to-weight ratios, lightweight, magnetic insensitivity, ease of handling, and flexibility to

fabricate laminates and/or lamina of desired strength and stiffness have helped the emergence of fiber-reinforced polymers (FRPs) as a potential future construction material in the construction industry.

Since the inception of reinforced concrete bridges in the U.S., the importance and use of concrete box-beam bridges have been gradually increased. Moreover, the technology and use of post-tensioned concrete box-beam bridges³ have progressed at a remarkable rate in the U.S. In addition, precast prestressed concrete members are being widely used in the construction of modern bridges⁴ due to their constructional, structural, and field advantages. Some of the distinctive advantages⁴ of using box-beam sections are: 1) small depth in comparison to the other shapes; 2) their monolithic construction imparts structural stability as well as enhanced appearance; 3) the hollow portion inside the concrete provides an ideal and safe space for utilities like gas lines, water pipes, telephone ducts, storm drains, sewers etc. to pass through bridges; 4) the high torsional stiffness of box-beam sections makes them ideal for the curvilinear and segmental bridges; and 5) the low depth-to-span ratio of box sections gives them a slender and aesthetically pleasing appearance. Apparently, there is no research literature on the structural response of box-beam bridges prestressed and reinforced using FRP tendons/strands. For the sake of background material and for easy understanding of the flexural response of box-beam bridges, a few of the most recent publications on the flexural response of beams prestressed using both bonded and unbonded FRP tendons are discussed below.

Iwamoto et al.⁵ suggested that the flexural behavior and ultimate strength of FRP prestressed concrete can be estimated by a conventional prestressed concrete analysis. Based on a study on the flexural characteristics of concrete beams prestressed using bonded pretensioning and unbonded CFRP tendons, Kato and Hayashida⁶ concluded that the failure of bonded CFRP prestressed concrete beams was brittle, whereas the beams prestressed with unbonded CFRP tendons had roughly the same degree of ductility as that of beams reinforced with steel strands.

Naaman et al.⁷ evaluated partially prestressed T-beams with CFCC and reported that the nonprestressed reinforcement imparted residual strength and ductility to the structure. Grace and Sayed⁸ studied the flexural behavior of double-tee (DT) beam bridges prestressed using bonded and external

ACI Structural Journal, V. 103, No. 1, January-February 2006.

MS No. 04-393 received December 13, 2004, and reviewed under Institute publication policies. Copyright © 2006, American Concrete Institute. All rights reserved, including the making of copies unless permission is obtained from the copyright proprietors. Pertinent discussion including author's closure, if any, will be published in the November-December 2006 *ACI Structural Journal* if the discussion is received by July 1, 2006.

ACI member **Nabil F. Grace** is a professor and Chair of the Civil Engineering Department and Director of the Center for Innovative Materials Research (CIMR), Lawrence Technological University (LTU), Southfield, Mich. He is a member of ACI Committee 440, Fiber Reinforced Polymer Reinforcement, and Joint ACI-ASCE Committee 343, Concrete Bridge Design.

Tsuyoshi Enomoto is a project engineer at Tokyo Rope Manufacturing Co., Ltd., Tokyo, Japan. He received his bachelor's degree in civil engineering from Kyushu Institute of Technology, Japan, in 1987. His research interests include bridges and concrete structures and he is actively involved in providing engineering support for CFRP cable-related projects.

Saju Sachidanandan is a structural engineer at NTH Consultants, Mich. He received his MSCE from LTU in 2005. His research interests include construction of underground structures.

Sreejith Puravankara is a structural engineer. He received his MSCE from LTU in 2005. His research interests include concrete rehabilitation using FRP, structural modeling, and elastic analysis.

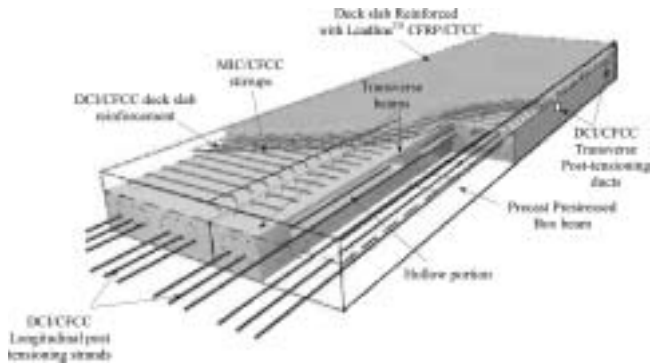


Fig. 1—Typical box-beam bridge model reinforced and prestressed with CFRP-DCI tendons/CFCC strands.

unbonded post-tensioning CFRP tendons with and without repeated load effects and concluded that repeated load had no significant effect on the external post tensioning strands. Maissen and de Semet⁹ evaluated the comparative response of concrete beams prestressed using bonded and unbonded CFRP tendons and the beams prestressed with bonded steel strands. The authors concluded that the beams prestressed with bonded and unbonded CFRP tendons demonstrated a higher flexural load carrying capacity than the beam prestressed with bonded steel strands.

According to an investigation conducted on the structural ductility of concrete beams prestressed with AFRP, CFRP, and steel strands, Naaman and Jeong¹⁰ concluded that the beams prestressed with FRP tendons experienced considerably lower ductility than the beams prestressed with steel strands. Moreover, the authors proposed a new approach to calculate the ductility that can be applicable to both steel and FRP reinforced/prestressed structures. A new construction approach^{11,12} for multi-span CFRP prestressed concrete bridges demonstrated that external post-tensioning using continuous draped tendons, continuous CFRP-reinforced deck slab, and transverse post-tensioning enhanced the ductility of the bridge model. Taniguchi et al.¹³ examined the flexural response of concrete beams prestressed using CFRP and AFRP tendons and concluded that the use of CFRP as transverse reinforcement increased the ductility of the beams.

A parametric study was conducted by Grace and Singh¹⁴ using a developed nonlinear computer program based on the strain controlled approach. It was concluded that the ultimate flexural strength and failure modes of DT beams prestressed using multi-layered pretensioning and external post-tensioning CFRP tendons depend on the level of initial

pretensioning and post-tensioning forces. Recently, Ng¹⁵ experimentally and theoretically examined the tendon stress and flexural strength of externally prestressed beams and concluded that the beam-span had no significant effect on the stress increase in external tendons. This result contradicts with the concluding remark of Naaman and Alkhairi.¹⁶

The objective of the present investigation is to develop, construct, instrument, and test two identical pairs of precast prestressed concrete box-beam bridge models, one reinforced using bonded pretensioning and unbonded post-tensioning CFRP-DCI tendons, and the other reinforced using bonded pretensioning and unbonded post-tensioning CFCC strands. The present study also addresses the parameters such as transfer lengths of CFRP-DCI tendons and CFCC strands, load-deflection and load-strain responses of the bridge models, and the comparison of ultimate load carrying capacities and failure modes of the two adjacent box-beam Bridge Models BBD-I and BBC-I.

RESEARCH SIGNIFICANCE

The experimental study presented in this paper explains the construction techniques employed for the adjacent box-beam bridge models using CFRP-DCI/CFCC bonded pretensioning and unbonded post-tensioning tendons/strands. This investigation also establishes the adequacy of using CFRP-DCI tendons and CFCC strands for the construction of highway bridges. Moreover, the results presented in the paper should be directly useful to designers for the selection of CFRP materials to meet their specific design requirements and to overcome the corrosion related problems in the current practice of highway box-beam bridges.

CONSTRUCTION DETAILS

Two adjacent box-beam bridge models, each consisting of two precast prestressed box beams, were constructed, instrumented, and tested. The two box beam bridge models were designated as BBD-I and BBC-I, depending upon the type of tendons/strands used for reinforcing and prestressing the box-beams of the bridge models. The box-beams used for the construction of Bridge Model BBD-I (BBD-I-1 and BBD-I-2) were reinforced and prestressed using CFRP-DCI tendons, whereas the box-beams of Bridge Model BBC-I (BBC-I-1 and BBC-I-2) were reinforced and prestressed using CFCC strands. The box-beams used in the construction of adjacent box-beam bridge models were 6.1 m (20 ft) long, 965 mm (38 in.) wide, and 229 mm (9 in.) deep.

Figure 1 shows the components of the developed CFRP reinforced and prestressed adjacent box-beam bridge model used in this investigation. In each bridge model, 14 prestressing tendons/strands, 12 post-tensioning tendons/strands, and 22 non-prestressing tendons/strands were used as flexural reinforcement. Figure 2 and 3 show the cross section and longitudinal section details of box-beam Bridge Model BBD-I with a 76 mm (3 in.) deck slab cast over the prestressed adjacent box-beams. The cross sections and longitudinal sections of the two bridge models (BBC-I and BBD-I) were identical except for the type of reinforcement used for reinforcing and prestressing. As shear reinforcement, MIC¹⁷ C-bar stirrups having a diameter of 9.5 mm (0.375 in.) were used in the construction of Bridge Model BBD-I, whereas CFCC 1 × 7, 7.5 mm-diameter stirrups were used in Bridge Model BBC-I.

Each box-beam of the two bridge models consisted of two hollow rectangular portions (Fig. 2) formed using commercially

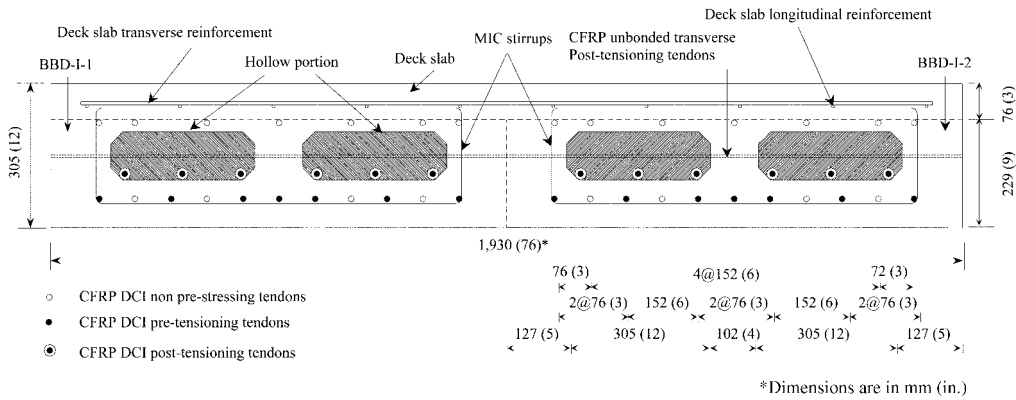


Fig. 2—Details of cross section of adjacent CFRP-DCI prestressed box-beam Bridge Model BBD-I.

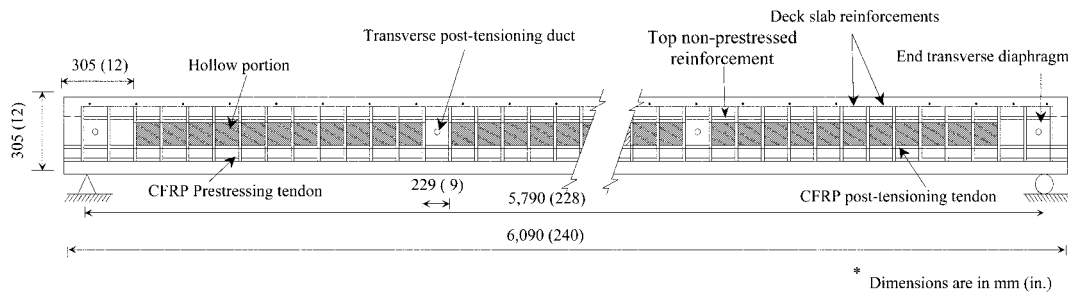


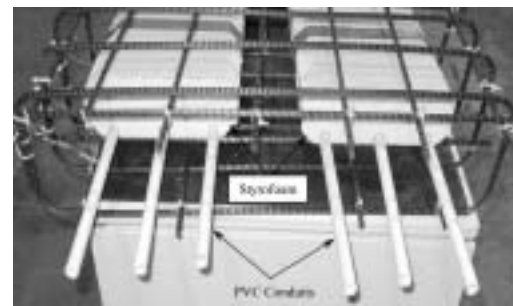
Fig. 3—Details of longitudinal section of box-beam Bridge Model BBD-I.

Table 1—Properties of MIC C-bar¹⁷ stirrups, CFRP-DCI tendons,¹⁸ and LeadlineTM tendons,¹⁹

Type of tendon/bar	MIC C-bar stirrups	CFRP-DCI tendons	Leadline TM tendons
Nominal diameter d , mm (in.)	9.5 (0.374)	9.5 (0.374)	8 (0.31)
Cross-sectional area, mm ² (in. ²)	71 (0.11)	71 (0.11)	46 (0.071)
Specified tensile strength, MPa, (ksi)	1896 (275)	1930 (280)	2268 (329)
Ultimate tensile strength, MPa, (ksi)	—	2103 (305)	—
Elastic modulus, GPa (ksi)	110 (16,000)	131 (19,000)	147 (21,320)
Specified ultimate tensile strain, %	1.7	1.47	1.5

Note: 1 MPa = 0.145 ksi; 1 kN = 0.225 kip; 1 g/m = 0.000672 lb/ft.

available Styrofoam. The width and depth of each hollow section were 305 and 102 mm (4 and 12 in.), respectively. Moreover, each box-beam was provided with four rectangular transverse diaphragms (Fig. 3), that is, one at each end of the box-beam and two at intermediate sections symmetrically located about the mid-span of the beam to facilitate the transverse post-tensioning of the bridge models. The reinforcement cage for Bridge Model BBD-I consisted of MIC C-bar stirrups and CFRP-DCI tendons (Fig. 4(a)), whereas the reinforcement cage for Bridge Model BBC-I consisted of CFCC stirrups and CFCC strands (Fig. 4(b)). To avoid premature shear failure and thereby allow the bridge models to fail in flexure, stirrups for each box-beam were provided at a spacing of 102 mm (4 in.). As shown in Fig. 4, each box-beam was also provided with six PVC conduits in the longitudinal direction and four PVC conduits in the transverse direction to accommo-



(a)



(b)

Fig. 4—(a) CFRP; and (b) CFCC reinforcement cages with Styrofoam and PVC conduits to facilitate unbonded post-tensioning tendons/strands.

date the longitudinal and transverse post-tensioning tendons/strands, respectively. The material properties of DCI tendons, MIC stirrups, LeadlineTM tendons, CFCC strands, and CFCC stirrups used in the construction of box-beam Bridge Models BBD-I and BBC-I are provided in Table 1 and 2.

Prior to placing of the reinforcement cage inside the formwork, seven tendons/strands were passed through the cage for subsequent pretensioning. In addition, seven nonprestressing tendons/strands at the top and four nonprestressing tendons/



Fig. 5—CFCC reinforcement cage placed in formwork along with pretensioning strands for casting two box-beams for Bridge Model BBC-I.

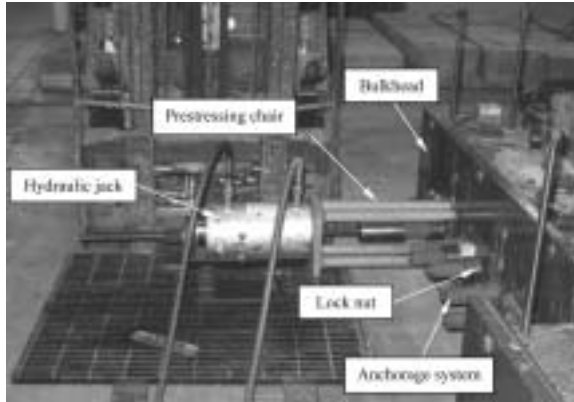


Fig. 6—Pretensioning of CFRP-DCI tendons using center-hole hydraulic jack.

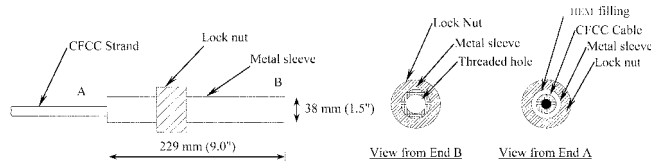


Fig. 7—Anchorage details of CFCC prestressing strands.



Fig. 8—Placing of concrete and use of vibrating equipment for proper compaction of concrete in Box Beams BBC-I-1 and BBC-I-2 of Bridge Model BBC-I.

strands located at the level of pretensioning were also provided as shown in Fig. 4. Moreover, all the pretensioning tendons/strands were instrumented with strain gauges to monitor the level of prestressing forces. An arrangement was made for the production of two prestressed box-beams of each bridge model

Table 2—Properties of prestressing and nonprestressing CFCC strands and stirrups²⁰

Type of strand	CFCC 1 x 7 stirrups	CFCC 1 x 7 prestressing/nonprestressing strands
Material characteristics		
Standard diameter d , mm (in.)	7.5 (0.3)	12.5 (0.49)
Measured diameter, mm (in.)	8.4 (0.33)	12.7 (0.50)
Effective cross-sectional area, mm ² (in. ²)	30 (0.047)	76 (0.12)
Pitch, mm (in.)	84 (3.3)	154 (6.1)
Linear density, g/m (lb/ft)	65 (0.0437)	153 (0.102)
Guaranteed breaking load, kN (kips)	57 (12.8)	142 (31.9)
Standard guaranteed strength, MPa (ksi)	1875 (272)	1868 (271)
Maximum value of measured breaking load, kN (kips)	71 (16.0)	188 (42.2)
Minimum value of measured breaking load, kN (kips)	65 (14.6)	181 (40.7)
Number of test specimens	5	8
Average measured breaking load, kN (kips)	67 (15.1)	183 (41.1)
Measured tensile strength, MPa (ksi)	2220 (322)	2410 (350)
Measured elastic modulus, GPa (ksi)	141 (20,450)	142 (20,595)
Ultimate strain, %	1.6	1.7

Note: 1 MPa = 0.145 ksi; 1 kN = 0.225 kip; 1 g/m = 0.000672 lb/ft.

simultaneously and is shown in Fig. 5. Furthermore, to monitor the prestressing force and to eliminate any possible instrumentation errors, load cells were attached at the dead ends of bulkheads. The required concrete cover of 51 mm (2 in.) at the bottom of box-beams was achieved by placing 102 mm (4 in.) diameter plastic circular chairs under the cage.

Prestressing

Each box-beam of the bridge models was prestressed using seven pretensioning CFRP-DCI tendons/CFCC strands. The prestressing system (Fig. 6) consisted of a long stroke center-hole jack, a hydraulic pump with pressure gauge, prestressing chair, a threaded steel tensioning rod, and a coupler. Jacking force was monitored using the pressure gauge of the hydraulic pump and load cells readings. It should be noted that the anchorage system for the CFRP-DCI tendons was attached to the ends of each prestressing tendon during the construction of the bridge model, while that for CFCC strands (Fig. 7) was preinstalled on the strands. Each pretensioning CFRP-DCI tendon used in the construction of the box-beams of Bridge Model BBD-I was stressed to an average of 45.4 kN (10.2 kips), thereby applying a total of 317.8 kN (71.4 kips) of pretensioning force to each box-beam. In Bridge Model BBC-I, each pretensioning CFCC strand was stressed to an average force of 44.3 kN (9.95 kips), thus constituting a total of 309.8 kN (69.7 kips) of pretensioning force for each box-beam.

After prestressing, the concrete was placed in the formwork (Fig. 8). During the concrete placement, special care was taken to protrude the stirrups beyond the top flange of the box-beams to provide shear connection with the deck slab (Fig. 9). After placing concrete, the box-beams were wet-cured using soaked burlap for 7 days. When the concrete attained the desired compressive strength, a saw-cut approach was used to transfer the pretensioning forces to



Fig. 9—CFCC shear stirrups protruding from box beams of Bridge Model BBC-I.



Fig. 10—Filling of gap between Box Beams BBD-I-1 and BBD-I-2 of Bridge Model BBD-I with structural concrete.

concrete simultaneously from both ends of the box beams. The 28-day compressive strength of concrete in the box beams of Bridge Models BBD-I and BBC-I were 50.3 and 57.2 MPa (7.3 and 8.3 ksi), respectively.

Construction of bridge models

Individual precast prestressed box beams were moved to the testing area underneath the loading frame and were placed adjacent to each other with simple supports at their ends. The adjacent arrangement of box beams provided a solid platform for initial post-tensioning application. The gap between the two adjacent box beams in each bridge model was grouted²¹ (Fig. 10). After curing the grout, an initial transverse post tensioning force was applied in each of the four transverse post-tensioning tendons/strands passing through the corresponding transverse diaphragms of the box beams. The transverse post-tensioning was necessary to maintain structural integrity of the two adjacent box beams and to prevent any differential movement during longitudinal post-tensioning, casting of deck slab, and application of external loads. Initial transverse post-tensioning consisted of applying 50% of the design transverse post-tensioning force (44.5 kN [10 kips]). After the initial transverse post-tensioning, initial longitudinal post-tensioning force was applied in unbonded longitudinal tendons/strands. The degree of initial longitudinal post-tensioning force was about 10% of total design post-tensioning force (89 kN [20 kips]). The final transverse and longitudinal post-tensioning forces were applied after the completion of the construction of CFRP/CFCC reinforced deck slab.

Construction of deck slab

As deck slab reinforcement, square grids of 203 x 203 mm (8 x 8 in.), using 8 mm (0.3 in.) diameter Leadline™ tendons¹⁹ (for Bridge Model BBD-I)/7.5 mm (0.3 in.) CFCC strands (for Bridge Model BBC-I), were fabricated and placed over the box beams and tied to protruded stirrups (Fig. 11). After attaching the reinforcement grid, a 76 mm (3 in.) deck slab was cast in the prepared formwork. The 28-day compressive strength of deck slab concrete for Bridge Models BBD-I and BBC-I were 53.8 and 42.7 MPa (7.8 and 6.2 ksi), respectively. The final transverse and longitudinal post-tensioning forces, which constitute about 50 and 90% of the design post-tensioning forces, respectively, were applied after the deck slab concrete attained the desired compressive strength.



Fig. 11—CFCC reinforcement cage placed in deck slab formwork of Bridge Model BBC-I.



Fig. 12—Arrangement of linear motion transducers and strain gauges before testing of Bridge Model BBD-I.

INSTRUMENTATION AND TEST SETUP

Concrete strains and deflections of the bridge models were monitored by installing strain gauges and linear motion transducers at specific locations. The arrangement of the linear motion transducers and strain gauges of Bridge Model BBD-I is shown in Fig. 12. The arrangement of sensors was similar for both bridge models for comparison. A total of five strain gauges were installed on concrete on either side of each bridge model at mid-span to measure strain during the application of external load. The lower and upper strain gauges were installed approximately 25 mm (1 in.) from the corresponding nearest edge, while the remaining four strain gauges were equally spaced over the remaining 254 mm

Table 3—Transfer lengths of CFRP-DCI tendons and CFCC strands of adjacent box-beam bridge models

Designated bridge model	Designated beams	Average prestress at transfer f_{pi} , MPa (ksi)	Precast concrete strength at transfer F'_{ci} , MPa (ksi)	Measured transfer length L_t , mm (in.)			Calculated transfer length L_t , mm (in.)		
				Live end	Dead end	Average	Eq. (1) (ACI 318) ²²	Eq. (2) (Grace) ²³	Eq. (3) (Zou) ²⁴
BBD-I	BBD-I-1	628.6 (91.2)	33.8 (4.9)	229 (9)	254 (10)	241 (9.5)	299 (11.8)	290 (11.4)	785 (30.9)
	BBD-I-2	636.6 (92.3)		305 (12)	254 (10)	279 (11)	302 (11.9)	306 (12.1)	785 (30.9)
BBC-I	BBC-I-1	565.6 (82.0)	42.1 (6.1)	279 (11)	254 (10)	267 (10.5)	354 (13.9)	307 (12.2)	925 (36.4)
	BBC-I-2	560.7 (81.3)		279 (11)	305 (12)	292 (11.5)	350 (13.8)	305 (12)	925 (36.4)

Note: 1 MPa = 0.145 ksi; 1 kN = 0.225 kip; 1 g/m = 0.000672 lb/ft.



Fig. 13—Test setup for box-beam Bridge Model BBD-I.

(10 in.) depth of the bridge model. In addition, five strain gauges were installed on the top surface of the deck slab. The strain gauges were symmetrically placed about the longitudinal mid-axis of the bridge model. To measure deflection of the bridge model, two linear motion transducers were installed at the mid-span, while one linear motion transducer was installed at each quarter-span location. Load cells installed at the dead ends of the longitudinal and transverse post-tensioning tendons/strands measured the post-tensioning forces in these tendons/strands. The data from all sensors were monitored and recorded using a 72-channel data acquisition system.

Flexural load tests were conducted to determine the ultimate load carrying capacity and ductility of the bridge models. The bridge models were single spanned and simply supported, consisting of a hinged support at one end and a roller support at the other end. The effective span of the box-beam bridge models was 5.79 m (19 ft). Load was applied to the bridge model through a loading frame, which was designed to distribute four-point load symmetrically. Loading and unloading cycles were continued until ultimate failure. These loading and unloading cycles were necessary to separate the elastic and inelastic energy of the models. All parameters such as deflections, top concrete strains, strains in pretensioned tendons/strands, forces in longitudinal and transverse post-tensioned tendons/strands, and actuator loading were monitored and recorded for all the loading and unloading cycles.

RESULTS AND DISCUSSION

In this section, the various parameters studied for investigating the flexural behavior of Bridge Models BBD-I and BBC-I are presented in detail. These include the transfer lengths of CFRP-DCI tendons and CFCC strands, the effect of concrete hardening on pretensioning forces, load-deflection

and load-strain responses, force variation in longitudinal unbonded post-tensioning tendons/strands, energy ratio, failure loads, and modes of failure of the two bridge models.

Transfer lengths

The transfer lengths of CFRP-DCI tendons and CFCC strands used to prestress box beams of Bridge Models BBD-I and BBC-I, respectively, are presented in Table 3. These transfer lengths are based on the saw-cut release of prestressing forces 7 days after the placement of concrete. The 7-day compressive strengths of concrete of the two box beams of Bridge Models BBD-I and BBC-I were 33.8 and 42.1 MPa (6.1 and 4.9 ksi), respectively. Transfer lengths were determined from the strain distribution along the length of beams near the ends using 95% average maximum strain method for 100% release of prestressing forces.²² It was determined that the measured transfer lengths at live and dead ends of the box-beams were in close agreement (Table 3). Moreover, the average value of the measured transfer length for 9.5 mm (0.374 in.) diameter CFRP-DCI tendons was about 27.4 times the nominal diameter of tendons, whereas the average values of the measured transfer length for the 12.5 mm (0.49 in.) diameter CFCC strands was about 22.4 times the nominal strand diameter. The difference in transfer length values of CFRP-DCI tendons and CFCC strands is attributed to the difference in compressive strength of concrete in the bridge models at transfer and also to the dissimilar geometric configuration (surface indentations) of CFRP-DCI tendons and CFCC strands. In Table 3, the calculated transfer lengths obtained using Grace,²² ACI 318-02,²³ and Zou²⁴ equations (Eq. (1) through (3), respectively) are presented. It was observed that the measured transfer lengths were close to that predicted by the Grace²² and ACI 318-02²³ equations; however, the measured transfer lengths are significantly lower than that predicted by the Zou²⁴ equation. Furthermore, these results contradict the concluding remarks of Zou,²⁴ who states that for all practical purposes, the effect of prestress on transfer length of tendons can be neglected and the transfer length should solely be based on Eq. (3) (modified version of BS 8110-1:1997²⁵).

$$L_t = \frac{f_{pi}d_b}{\alpha_t f'_{ci}{}^{0.67}} \text{ (Grace}^{22}\text{)} \quad (1)$$

$$L_t = \frac{f_{pi}d_b}{20} \text{ (ACI 318-02}^{23}\text{)} \quad (2)$$

$$L_t = \frac{480d_b}{\sqrt{f'_c}} \text{ (Zou}^{24}\text{)} \quad (3)$$

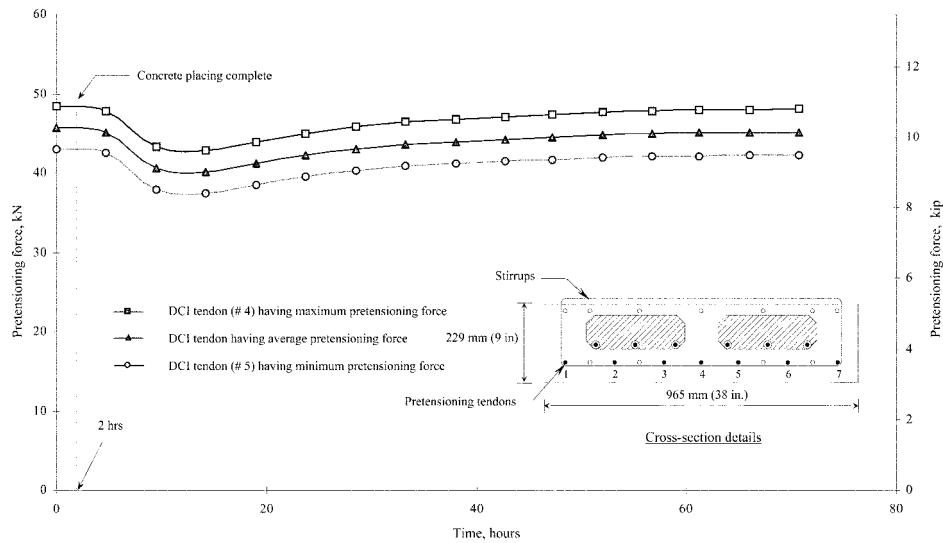


Fig. 14—Changes in pretensioning force of CFRP-DCI tendons during and after placement of concrete in formwork of Box Beam BBD-I-1.

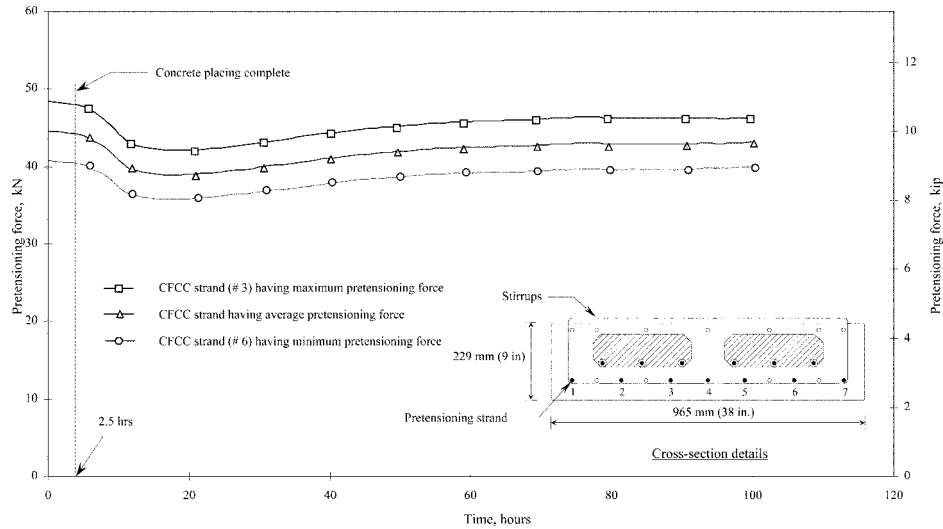


Fig. 15—Changes in pretensioning force of CFCC strands during and after placement of concrete in formwork of Box Beam BBC-I-1.

where d_b is the nominal diameter of tendon/strand (mm), f_{pi} is the prestress at transfer (MPa); f'_{ci} is the strength of concrete at transfer (MPa); and α_t is the transfer length coefficient, where $\alpha_t = 1.95$ for CFRP tendons¹⁹ and 2.12 for CFCC strands. Note that for CFRP-DCI tendons, the factor α_t was taken as 1.95 because of similar geometric configuration as of the Leadline™ tendons.¹⁹

Effect of concrete hardening on pretensioning forces

As shown in Fig. 14 and 15, the forces in pretensioning tendons/strands, as measured by the load cells, rapidly decreased after the placement of concrete in the formwork. This apparent loss in the prestressing forces is attributed to the concrete hydration process. Due to the expansion of concrete and tendon, the load cells at the dead end of abutment partially lost contact with the abutment. This marginal loss of contact between load cells and abutment resulted in the apparent loss in pretensioning forces. However, this apparent loss in the pretensioning forces of both CFRP-DCI tendons

and CFCC strands was gradually restored within two days (48 hours) subsequent to the placement of concrete. The restoration of pretensioning forces was due to the shrinkage of concrete during curing, which reestablished the contact of the load cells with the abutment. This result signifies the importance of curing of concrete in prestressed beams and cautions against the early release of prestress.

Load-deflection response and variation of forces in unbonded tendons/strands

The ultimate load-deflection responses of the two Bridge Models BBD-I and BBC-I are shown in Fig. 16. Several loading and unloading cycles were performed on the bridge models to separate the inelastic energy absorbed and the elastic energy released until the failure. The point on the load deflection curves (Fig. 16) corresponding to the change in slope defines the cracking load and is attributed to the change in stiffness of the section after cracking. The values of cracking load corresponding to the appearance of the first

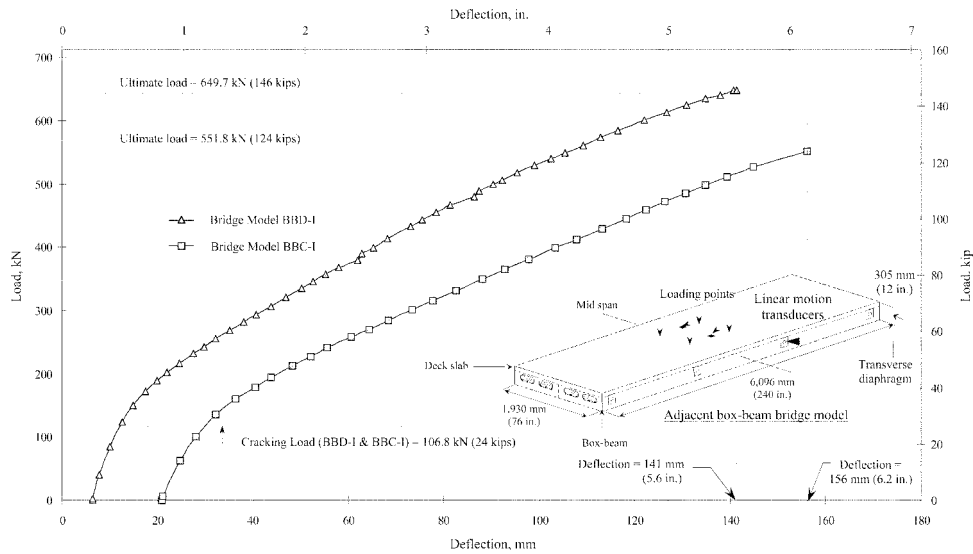


Fig. 16—Ultimate load-deflection responses at midspan of Bridge Models BBD-I and BBC-I after loading and unloading cycles.

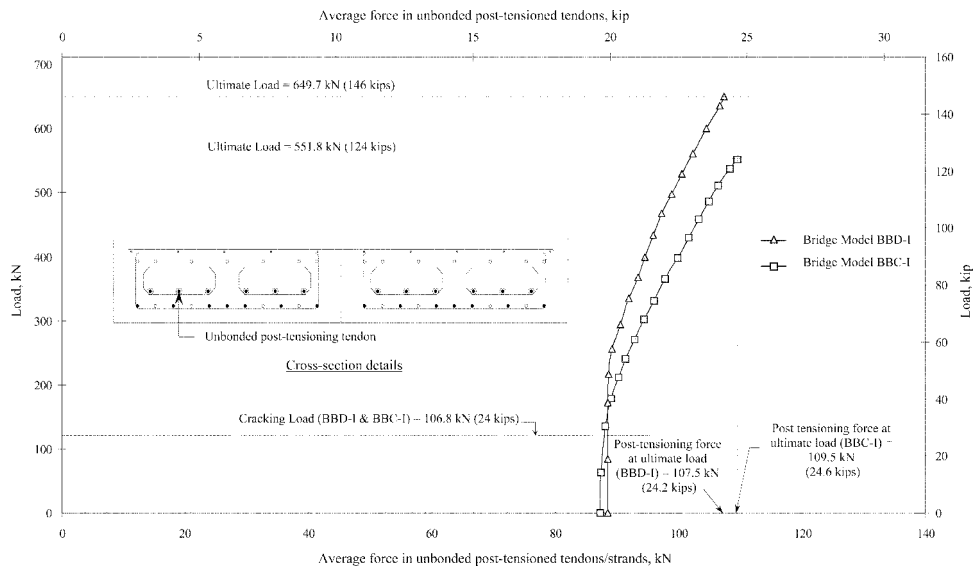


Fig. 17—Load versus average force in longitudinal unbonded post-tensioning tendons/strands of Bridge Models BBD-I and BBC-I.

crack in the box beams of Bridge Models BBD-I and BBC-I were observed to be the same, that is, 106.8 kN (24 kips). Moreover, it was determined that the ultimate load-carrying capacities of Bridge Models BBD-I and BBC-I at failure were about 649.7 and 552 kN (146 and 124 kips), respectively, and the corresponding deflections were 142 and 156 mm (5.6 and 6.2 in.), respectively.

The variation of forces in unbonded post-tensioning tendons/strands of Bridge Models BBD-I and BBC-I with respect to the applied load is shown in Fig. 17. After cracking, the forces in the unbonded post-tensioning tendons of Bridge Model BBD-I at a particular applied load was slightly higher than that of Bridge Model BBC-I. At ultimate load, average increases of 18.9 and 22.3 kN (4.3 and 5 kips) were experienced in longitudinal unbonded post-tensioning tendons/strands of Bridge Models BBD-I and BBC-I, respectively. Moreover, it was observed that all unbonded post-tensioning tendons/strands remained intact even after the ultimate failure of the bridge models. It should also be

noted that the load carrying capacity of the bridge models dropped significantly even though the internal unbonded post-tensioning tendons/strands remained intact after failure. Furthermore, the variation of forces in the transverse unbonded post-tensioning tendons/strands was negligible.

Failure mode of bridge models

Both Bridge Models BBD-I and BBC-I experienced flexural failure. The failure was initiated by the crushing of concrete in the compression zone followed by the rupture of pretensioning tendons/strands (Fig. 18 and 19). This failure mode was anticipated, as both bridge models were over-reinforced. Moreover, Bridge Model BBD-I experienced a 17% higher ultimate load carrying capacity than that of Bridge Model BBC-I, which is due to the higher concrete compressive strength (about 44%) in the compression zone (deck slab) of Bridge Model BBD-I as the failure is initiated by the crushing of concrete in the compression zone.



Fig. 18—Flexural failure of Bridge Model BBD-I.



Fig. 19—Flexural failure of Bridge Model BBC-I.

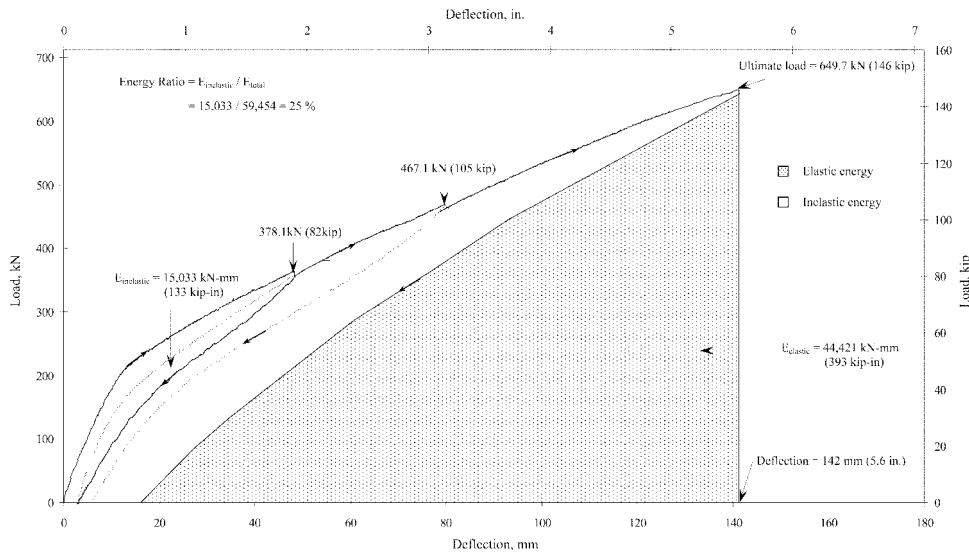


Fig. 20—Energy ratio of Bridge Model BBD-I.

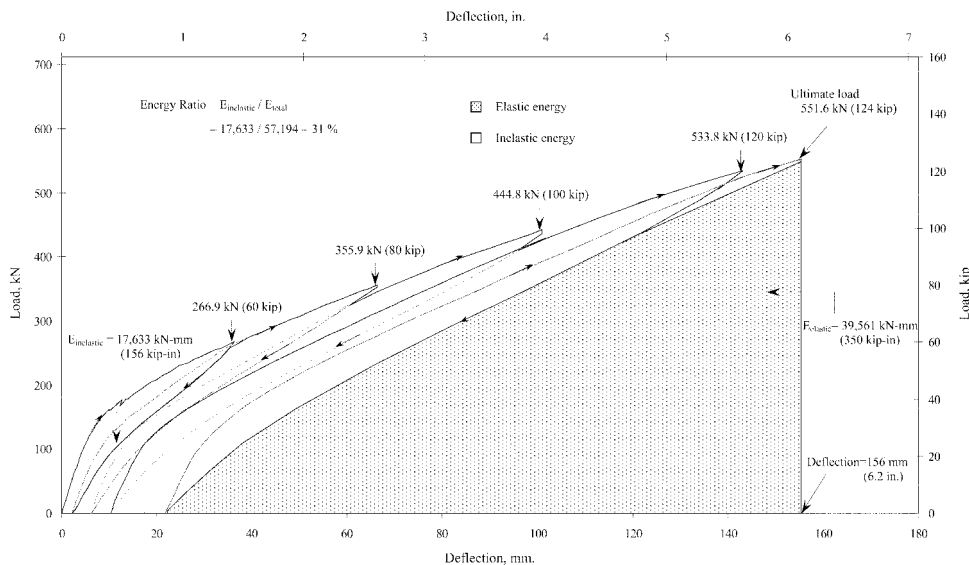


Fig. 21—Energy ratio of Bridge Model BBC-I.

Ductility of bridge models

The ductility of adjacent box-beam Bridge Models BBD-I and BBC-I was determined by evaluating the released elastic energy and the absorbed inelastic energy until the failure. The ductility of the bridge models is expressed by the energy ratio, that is, the ratio of inelastic energy absorbed to the total energy.^{8,10} To measure the energy ratio, each bridge model was

subjected to several loading-unloading cycles. Figure 20 and 21 show the load-deflection curves used to compute the energy ratio of the bridge models. The final unloading curve was obtained by simulating the unloading curve for the second last cycle. The computed energy ratios of Bridge Models BBD-I and BBC-I were approximately 25 and 31%, respectively, which were considered rather brittle, and hence indicates the need to explore

other design philosophies to improve the ductility of CFRP/CFCC reinforced and prestressed concrete box-beam bridge models.

CONCLUSIONS

Based on the experimental data obtained from this investigation, it is concluded that both Bridge Models BBD-I and BBC-I demonstrated identical flexural behavior, especially the cracking load, mode of failure, and variation in post-tensioning forces. Furthermore, the following conclusions are drawn.

The average value of the measured transfer lengths of 9.5 mm (0.374 in.) diameter CFRP-DCI tendons is about 27.4 times the nominal diameter of tendons, whereas that of the 12.5 mm (0.49 in.) diameter CFCC strands is about 22.4 times the nominal strand diameter. The transfer length equations of Grace²² and ACI 318-02²³ closely estimate the measured transfer lengths of CFRP-DCI tendons and CFCC strands. Comparison of calculated transfer lengths using various equations with measured transfer lengths indicates that the effect of prestress on transfer length cannot be ignored.

The apparent loss of prestress due to heat generated during curing of concrete suggests that pretensioning forces should not be released until at least 2 days after the casting of concrete. Hence, early release of pretensioning force is not advised.

The cracking loads of the two Bridge Models BBD-I and BBC-I are observed to be approximately 106.8 kN (24 kips). Moreover, Bridge Model BBD-I experienced 17% higher ultimate load carrying capacity than that of Bridge Model BBC-I, which is attributed to the higher concrete compressive strength in the compression zone (deck slab) of Bridge Model BBD-I, as the failure was initiated by the crushing of concrete in the compression zone.

After cracking, the increase in post-tensioning forces of unbonded tendons of Bridge Model BBD-I at a particular applied load was slightly higher than that of Bridge Model BBC-I. Moreover, at ultimate load, average increases of 18.9 and 22.3 kN (4.3 and 5.0 kips) were experienced in longitudinal unbonded post-tensioning tendons/strands of Bridge Models BBD-I and BBC-I, respectively. Furthermore, it is noted that all longitudinal unbonded post-tensioning tendons/strands of the two bridge models remained intact even after failure.

The failure of both Bridge Models BBD-I and BBC-I was initiated by crushing of concrete in the compression zone followed by the rupture of pretensioning tendons/strands, as both bridge models were over-reinforced. The energy ratios obtained for Bridge Models BBD-I and BBC-I were 25 and 31%, respectively, which indicates the need to explore other design features to improve the ductility of developed CFRP/CFCC reinforced and prestressed concrete box-beam bridge systems.

ACKNOWLEDGMENTS

This investigation was supported by a consortium of the National Science Foundation (Grant No. CMS-0533260 and CMS-0408593); the Tokyo Rope Manufacturing Co. Ltd., Japan; the ACI Concrete Research Council; Diversified Composites, Inc., which manufactured the CFRP-DCI tendons; and Mitsui Co., Japan. The CFRP Leadline prestressing rods were manufactured by the Mitsubishi Chemical Co., Japan. This experimental study was made possible through the efforts of several research associates and graduate and undergraduate students. The contributions of S. B. Singh, post-doctoral Research Fellow at LTU, are highly appreciated, as are the technical comments of Roger Till of MDOT.

REFERENCES

1. Naaman, A. E., and Chandrangsu, K., "Innovative Bridge Deck System Using High-Performance Fiber-Reinforced Cement Composites," *ACI Structural Journal*, V. 101, No. 1, Jan.-Feb. 2004, pp. 57-64.

2. ACI Committee 440, "State-of-the-Art Report on Fiber Reinforced Plastic Reinforcement for Concrete Structures (ACI 440R-96) (Reapproved 2002)," American Concrete Institute, Farmington Hills, Mich., 1996, 65 pp.
3. Hindi, A.; MacGregor, R.; Kreger, M. E.; and Breen, J. E., "Enhancing Strength and Ductility of Post-Tensioned Segmental Box Girder Bridges," *ACI Structural Journal*, V. 92, No. 1, Jan.-Feb. 1995, pp. 73-94.
4. Taly, N., *Design of Modern Highway Bridges*, McGraw Hill Co., Inc., New York, 1998, pp. 382-487.
5. Iwamoto, K.; Uchita, Y.; Takagi, N.; and Kojima, T., "Flexural Fatigue Behavior of Prestressed Concrete Beams Using Aramid-Fiber Tendons," *International Symposium on Fiber-Reinforced-Plastic Reinforcement for Concrete Structures*, SP-138, A. Nanni and C. W. Dolan, eds., American Concrete Institute, Farmington Hills, Mich., 1993, pp. 509-523.
6. Kato, T., and Hayashida, N., "Flexural Characteristics of Prestressed Concrete Beams with CFRP Tendons," *International Symposium on Fiber-Reinforced-Plastic Reinforcement for Concrete Structures*, SP-138, A. Nanni and C. W. Dolan, eds., American Concrete Institute, Farmington Hills, Mich., 1993, pp. 419-440.
7. Namaan, A. E.; Tan, K. H.; Jeong, S. M.; and Alkhalil, F. M., "Partially Prestressed Beams with Carbon Fiber Composite Strands: Preliminary Tests Evaluation," *International Symposium on Fiber-Reinforced-Plastic Reinforcement for Concrete Structures*, SP-138, A. Nanni and C. W. Dolan, eds., American Concrete Institute, Farmington Hills, Mich., 1993, pp. 441-464.
8. Grace, N. F., and Sayed, G. A., "Behavior of Externally/Internally Prestressed Composite Bridge System," *Proceedings of the 3rd International Symposium on Non-Metallic (FRP) Reinforcement for Concrete Structures*, V. 2, Sapporo, Japan, 1997, pp. 671-678.
9. Maissen, A., and de Semet, C. A. M., "Comparison of Concrete Beams Prestressed with Carbon Fiber-Reinforced Plastic and Steel Strands," *Non-Metallic (FRP) Reinforcement for Concrete Structures*, Proceedings of the 2nd International RILEM Symposium (FRPRCS), Ghent, Belgium, Aug. 1995, pp. 430-439.
10. Naaman, A. E., and Jeong, S. M., "Structural Ductility of Concrete Beams Prestressed with FRP Tendons," *Non-Metallic (FRP) Reinforcement for Concrete Structures*, Proceedings of the 2nd International RILEM Symposium (FRPRCS), Ghent, Belgium, Aug. 1995, pp. 379-386.
11. Grace, N. F.; Enomoto, T.; Abdel-Sayed, G.; Yagi, K.; and Collavino, L., "Experimental Study and Analysis of a Full-Scale CFRP/CFCC Double-Tee Bridge Beam," *PCI Journal*, V. 48, No. 4, Jul.-Aug. 2003, pp. 120-139.
12. Grace, N. F., "Response of Continuous CFRP Prestressed Concrete Bridges Under Static and Repeated Loadings," *PCI Journal*, V. 45, No. 6, Nov.-Dec. 2000, pp. 84-102.
13. Taniguchi, H.; Mutsuyoshi, H.; Kita, T.; and Machida, A., "Flexural Behavior of Externally Prestressed Concrete Beams Using CFRP and Aramid Rope Under Static and Dynamic Loading," *Proceedings of the 3rd International Symposium on Non-Metallic (FRP) Reinforcement for Concrete Structures*, V. 2, Sapporo, Japan, 1997, pp. 783-790.
14. Grace, N. F., and Singh, S. B., "Design Approach for Carbon Fiber-Reinforced Polymer Prestressed Concrete Bridge Beams," *ACI Structural Journal*, V. 100, No. 3, May-June 2003, pp. 365-376.
15. Ng, C.-K., "Tendon Stress and Flexural Strength of Externally Prestressed Beams," *ACI Structural Journal*, V. 100, No. 5, Sept.-Oct. 2003, pp. 644-653.
16. Naaman, A. E., and Alkhalil, F. M., "Stress at Ultimate in Unbonded Post-Tensioning Tendons: Part 2—Proposed Methodology," *ACI Structural Journal*, V. 88, No. 6, Nov.-Dec. 1991, pp. 683-692.
17. Marshall Industries Composites, Inc., "MIC Carbon Fiber C-Bars," *Carbon C-Bars Reinforcing Bar Product Specifications*, Lima, Ohio, 2000.
18. Diversified Composites, Inc., *DCI Tendon Product Specifications*, Erlanger, Ky., 2004 (www.Diversified-Composites.com).
19. Mitsubishi Chemical Corporation, "Leadline™ Carbon Fiber Tendons/ Bars," *Product Manual*, Minato-Ku, Tokyo, Japan, 1994.
20. Tokyo Rope Manufacturing Co. Ltd., "Technical Data on CFCC Strands," *Product Manual*, Tokyo, Japan, 1993, 100 pp.
21. Five Star Products Inc., *Users Manual for Five Star Structural Concrete*, Fairfield, Conn., 2002, 3 pp. (www.Fivestarp.com).
22. Grace, N. F., "Transfer Lengths of CFRP/CFCC Strands for DT-Girders," *PCI Journal*, V. 45, No. 5, 2000, pp. 110-126.
23. ACI Committee 318, "Building Code Requirements for Structural Concrete (ACI 318-02) and Commentary (318R-02)," American Concrete Institute, Farmington Hills, Mich., 2002, 443 pp.
24. Zou, P. X. W., "Long-Term Properties and Transfer Length of Fiber Reinforced Polymers," *Journal of Composites for Construction*, ASCE, V. 7, No. 1, Feb., 2003, pp. 10-19.
25. British Standards Institution (BSI), "Structural Use of Concrete: Code of Practice for Design and Construction," BS 8110-1:1997, London, 1997, 172 pp.